

LC/MS of Intact Adeno-Associated Virus Capsid Proteins for Rapid Confirmation of Product Identity

Author

Brian Liao
Agilent Technologies, Inc.

Introduction

Adeno-associated viruses (AAVs) are a promising new class of biotherapeutic capable of treating a host of rare and intractable genetic diseases such as spinal muscular atrophy and inherited retinal degeneration.¹ AAVs are large molecular complexes consisting of a protein capsid and encapsulated DNA, with each requiring dedicated analytical techniques to ensure the quality and safety of the overall product. AAV capsids comprise three different capsid proteins, commonly denoted VP1–3, in approximately a 1:1:10 stoichiometric ratio with a total of 60 copies of protein per capsid.²

The U.S. Food and Drug Administration recommends viral capsids and encapsulated DNA of all AAV therapeutics to be unambiguously identified before release, especially in facilities where multiple serotypes or engineered variants are produced.³ To date, antibody-based methods such as ELISA and immunoblotting have been the most common techniques for viral capsid analysis. These methods suffer from several drawbacks: in addition to being cumbersome and error-prone, antibody-based methods require highly specific antibodies to be generated for each type of AAV being analyzed. This is challenging because AAV capsids from different products may have a high degree of homology – for example, AAV serotypes 1 and 6 differ by only six amino acids (99% homology), making them difficult to distinguish by antibody binding.⁴

In principle, LC/MS offers the ideal combination of speed and specificity for viral capsid protein analysis because direct measurement of protein masses obviates the need to generate antibodies for each type of AAV. However, previous efforts have suffered from relatively poor chromatographic separation of virus capsid proteins.⁵ This is problematic because coelution may compromise signal intensity and mass accuracy, in addition to precluding accurate quantitation of capsid stoichiometry, which is an important determinant of AAV infectivity.⁶

This application note demonstrates an optimized LC/FLD-MS method for the rapid analysis of AAV capsid proteins to confirm the primary sequences of seven different serotypes. This method has simple sample preparation requirements and is robust to high salt conditions as well as the common nonionic detergent additive Pluronic F-68.

Experimental

AAV Samples

AAV serotypes 2, 7, 9, 7m8, DJ, rh10, and Anc80 were purchased from the Vector Core @ GIS (A*STAR, Singapore). AAV samples were expressed in HEK-293 cells by triple transfection and purified by analytical ultracentrifugation. Samples were provided at a concentration of $\sim 1.2 \times 10^{10}$ viral genomes/ μL in phosphate-buffered saline containing 0.001% Pluronic F-68 and used as received without buffer exchange.

Sample preparation

A denaturation buffer consisting of 12 M guanidine HCl + 40 mM DTT in 200 mM ammonium bicarbonate (pH ~ 8.0) was freshly prepared for each analysis. Denaturation buffer was added to AAV samples in a 1:3 ratio to achieve a final guanidine HCl concentration of 3 M. Samples were then heated to 70 °C for 15 minutes to ensure complete denaturation. 1.5×10^{11} viral genomes were injected per analysis.

LC/FLD-MS for intact capsid protein analysis

Samples were analyzed using the following instrumentation:

- Agilent 1290 Infinity II LC system including:
 - Agilent 1290 Infinity II High Speed Pump (G7120A)
 - Agilent 1290 Infinity II Multisampler (G7167B)
 - Agilent 1290 Infinity II Multicolumn Thermostat (G7116B)

- Agilent 1260 Infinity Fluorescence Detector (G1321B) with 8 μL flow cell
- Agilent 6545XT AdvanceBio LC/Q-TOF

For separation, Agilent ZORBAX RRHD 300Å StableBond C18 (SB-C18) and SB-Diphenyl columns with dimensions 2.1 \times 100 mm, 1.8 μm (part numbers 858750-902 and 858750-944) were used. A ZORBAX RRHD 300Å SB-C3 column (part number 858750-909) was also used for development, but not the optimized method.

A high eluotropic strength mobile phase consisting of 0.1% TFA + 0.1% FA in DI water (mp A) and 90% isopropyl alcohol + 9.8% water + 0.1% TFA + 0.1% FA (mp B) was chosen. In combination with high temperature, similar mobile phase conditions have achieved superior resolving power on ZORBAX StableBond columns for monoclonal antibody analysis.⁷

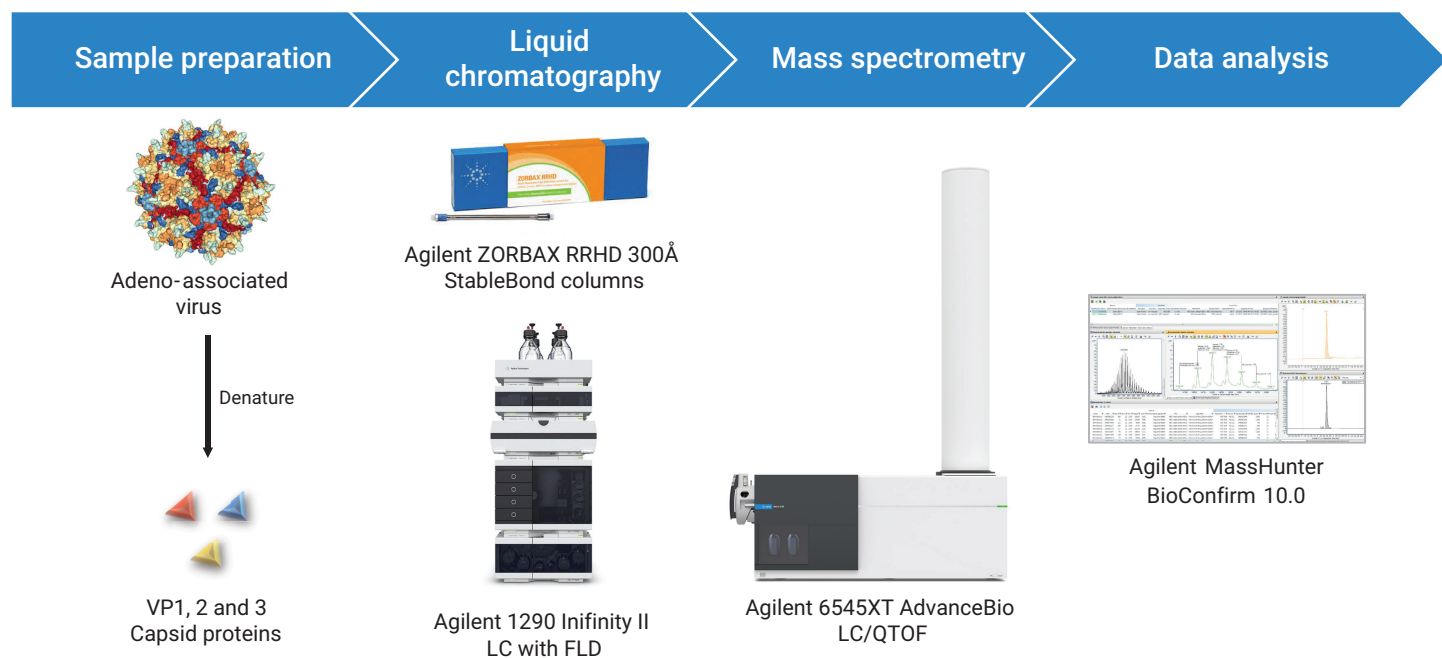


Figure 1. Equipment and consumables used in this application note.

For fluorescence detection, an 8 μL flow cell with single excitation (280 nm)/ multiple emission (315, 330, 345, and 360 nm) mode was used as the emission spectra of aromatic residues may vary depending on number and the degree of solvent exposure. Emission at 360 nm was found to be most intense and was therefore used for all analyses. All data analysis was carried out in Agilent BioConfirm 10.0. Tables 1, 2, and 3 show the instrument and software settings.

LC/MS peptide mapping analysis

A 10 μL amount of sample containing 6.0×10^{11} viral genomes of AAV 2 (~3.6 μg of protein) was denatured and reduced in 30 μL of 150 mM Tris-HCl (pH 8) containing 760 mg/mL guanidine HCl + 3.8 mg/mL TCEP for 60 minutes at 60 °C. After cooling to room temperature, alkylation was performed by adding 10 μL of 133 mM iodoacetamide and incubating at room temperature in darkness for 30 minutes. The sample was then diluted with 210 μL of Tris-HCl, after which 0.2 μg of Promega's Sequencing Grade Modified Trypsin (part number V5117) was added. Digestion was carried out for 2 hours at 37 °C, after which a further 0.2 μg of trypsin was added before digesting overnight at 37 °C. The following day,

Table 2. Intact capsid protein mass spectrometry parameters.

Agilent 6545XT AdvanceBio LC/Q-TOF System	
Source	Agilent Dual Jet Stream
Gas Temperature	350 °C
Gas Flow	12 L/min
Nebulizer	35 psig
Sheath Gas Temperature	350 °C
Sheath Gas Flow	11 L/min
Vcap	4 kV
Nozzle Voltage	2 kV
Fragmentor	180 V
Skimmer	65 V
Mass Range	900 to 3,200 m/z
Acquisition Rate	1 spectrum/sec
Reference Mass	922.0098
Acquisition Mode	Positive, 3,200 m/z mass range, Extended dynamic range (2 Ghz)

the reaction was stopped by adding 30 μL of 10% formic acid, followed by C-18 cleanup using an Agilent AssayMap Bravo system (G5542A).

Peptide mapping was performed on a 1290 Infinity II LC with 6545XT AdvanceBio LC/Q-TOF. An AdvanceBio Peptide Mapping column (part number 653750-902) with dimensions 2.1 \times 150 mm, 2.7 μm was used for separation. Tables 4 and 5 show the instrument settings.

Table 3. Intact capsid protein deconvolution settings.

Agilent MassHunter BioConfirm B10.0 Settings	
Defined Chromatograms	FLD
Integrate When Extracted	Yes
Adjust Delay Time	0.1 min (MS Detector)
Deconvolution	Maximum entropy
Deconvolution m/z Range	1,000 to 3,200
Deconvolution Mass Range	55 to 85 kDa
Mass Step	0.5 Da
Deconvolution Subtract Baseline	7.0
Match Tolerance	32 ppm

Table 4. Peptide mapping chromatographic parameters.

Agilent 1290 Infinity II LC System	
Solvent A	0.1% FA in DI water
Solvent B	0.1% FA in Acetonitrile
Gradient	0 to 15 min, 5 to 40% B 15 to 18 min, 40 to 90% B 18 to 20 min, 90% B
Column Temperature	60 °C
Flow Rate	0.4 mL/min
Injection Volume	20 μL

Table 1. Intact capsid protein chromatographic parameters.

Agilent 1290 Infinity II LC System						
Condition	Testing	Optimized	Testing	Optimized	Testing	Optimized
Column	Agilent ZORBAX RRHD 300Å StableBond C18, 2.1 \times 100 mm, 1.8 μm (p/n 858750-902)	Agilent ZORBAX RRHD 300Å StableBond Diphenyl, 2.1 \times 100 mm, 1.8 μm (p/n 858750-944)	Agilent ZORBAX RRHD 300Å StableBond Diphenyl, 2.1 \times 100 mm, 1.8 μm (p/n 858750-944)	Agilent ZORBAX RRHD 300Å StableBond Diphenyl, 2.1 \times 100 mm, 1.8 μm (p/n 858750-944)	Agilent ZORBAX RRHD 300Å StableBond C3, 2.1 \times 100 mm, 1.8 μm (p/n 858750-909)	Agilent ZORBAX RRHD 300Å StableBond C3, 2.1 \times 100 mm, 1.8 μm (p/n 858750-909)
Solvent A	0.1% FA+ 0.1% TFA in DI water	0.1% FA+ 0.1% TFA in DI water	0.1% FA+ 0.1% TFA in DI water	0.1% FA+ 0.1% TFA in DI water	0.1% FA+ 0.1% TFA in DI water	-
Solvent B	80% IPA + 10% ACN + 9.8% DI water + 0.1% FA + 0.1% TFA	90% IPA + 9.8% DI water + 0.1%FA + 0.1%TFA	80% IPA + 10% ACN + 9.8% DI water + 0.1% FA + 0.1% TFA	90% IPA + 9.8% DI water + 0.1%FA + 0.1% TFA	80% IPA + 10% ACN + 9.8% DI water + 0.1% FA + 0.1% TFA	-
Gradient	0 to 2 min, 20% B 42 min, 35% B 42.5 min, 80% B 45 min, 80% B	0 to 5 min, 28% B 23 min, 32.5% B 23.5 min, 80% B 26 min, 80% B	0 to 2 min, 28% B 42 min, 43% B 42.5 min, 80% B 45 min, 80% B	0 to 5 min, 33% B 21 min, 37% B 21.5 min, 80% B 23 min, 80% B	0 to 2 min, 20% B 42 min, 35% B 42.5 min, 80% B 45 min, 80% B	-
Column Temperature	75 °C	80 °C	75 °C	80 °C	75 °C	-
Flow Rate	0.4 mL/min					
Sample Quantity	1.5×10^{11} Viral genomes/injection					

Results and discussion

LC/MS method development

AAV-2 was used for method development as it is the most well-studied serotype. The sequences of capsid proteins VP1–3 are shown in Figure 2. All capsid proteins are transcribed from the same DNA sequence in the Cap gene, with mRNA splicing and leaky ribosomal scanning resulting in three proteins with a high degree of homology.⁶ Specifically, the VP3 sequence is common to all three proteins, with VP1 and VP2 differing only in their N-terminal sequences.

Table 5. Peptide mapping mass spectrometry parameters.

Agilent 6545XT AdvanceBio LC/Q-TOF System		Precursors/Cycle	Top 10
Source	Agilent Dual Jet Stream	Collision Energy	3.6*(m/z)/100 – 4.8
Gas Temperature	290 °C	Threshold for MS/MS	On; 3 repeat then exclude for 0.2 minutes
Gas Flow	13 L/min	Precursor Abundance-Based Scan Speed	Yes
Nebulizer	35 psig	Target	25,000
Sheath Gas Temperature	275 °C	Use MS/MS Accumulation Time Limit	Yes
Sheath Gas Flow	12 L/min	Purity	100% stringency, 30% cutoff
Vcap	4 kV	Isotope model	Peptides
Nozzle Voltage	2 kV	Sort precursors	By abundance only; +2, +3, >+3
Fragmentor	175 V	Reference mass	922.0098
Skimmer	65 V	Acquisition mode	Positive, 3,200 m/z mass range
Mass Range	100 to 1,700 m/z		
Acquisition Rate	5 spectra / sec		
Auto MS/MS Range	50 to 1,700 m/z		
Min. MS/MS Acquisition Rate	3 spectra / sec		
Isolation Width	Medium (~4 m/z)		

A:VP1 Monoisotopic mass: 81804.8749 Average mass: 81856.1324 Molecular formula: C3630H5483N1015O1127S15

```

1 N-term AADGYLPDWLEDTLSEGIRQWVKLKPPPPKPAERHKDDSRGLVLPGYKYLGPFNGLDKGEVPVNEADAAAEHDKAYDRQLDSDGNPYLYKNH 94
95 ADAEFQERLKEDTSFGGNLGRAVFOAKRVLEPLGLVEEPVKTAPGKKRPVEHSPVEPDSSSGTGKAGQQPARKRLNFGQTGDADSVDPDQPLGQPPAAPSGLG 198
199 TNTMATGSGAPMADNNEGADGVGNSSGNWHCDSTWMDRVIITSTRTWALPTYNNHLYKQISSQSGASNDNHYFGYSTPWGYDFNRFHCHFSPRDWQRLINNN 302
303 WGFRPKRLNFKLFNIQVKEVTQNDGTTIANNLTSTVQVFTDSEYQLPYVLGSAHQGCLPPFPADVFMVPOYGYLTLNNGSQAVGRSSFYCLEYFPSQMLRTGN 406
407 NFTFSYTFEDVPPHSSYAHSQSLDRLMNPLIDQYLYLSRTNTPSGTTTQSRLLQFSQAGASDIRDQSRNWLPGPCYRQQRVSKTSADNNNSEYSWTGATKYHLN 510
511 GRDSLVPNGPAMASHKDDEEKFFPQSGVLIFGKQSEKTNVDIEKVMITDEEEIRTTNPVATEQYGSVSTNLQQRNRQAATADVNTQGVLPGMVWQDRDVLVYQG 614
615 PIWAKIPHTDGHFHPSPLMGGFGLKHPPPQILIKNTVPPANPSTTFSAAKFASFITQYSTGQVSVEIEWELQKENSKRWNPEIQYTSNYNKSVMVDFTVDTNGV 718
719 YSEPRPIGTRYLTRNL C-term 734
  
```

B:VP2 Monoisotopic mass: 66447.1172 Average mass: 66488.9131 Molecular formula: C2938H4429N827O917S15

```

1 N-term APGKKRPVEHSPVEPDSSSGTGKAGQQPARKRLNFGQTGDADSVDPDQPLGQPPAAPSGLGTNTMATGSGAPMADNNEGADGVGNSSGNWHCD 94
95 TWMDRVIITSTRTWALPTYNNHLYKQISSQSGASNDNHYFGYSTPWGYDFNRFHCHFSPRDWQRLINNNWGFRPKRLNFKLFNIQVKEVTQNDGTTIANNL 198
199 TSTVQVFTDSEYQLPYVLGSAHQGCLPPFPADVFMVPOYGYLTLNNGSQAVGRSSFYCLEYFPSQMLRTGNNTFTFSYTFEDVPPHSSYAHQSLDRLMNPLIDQ 302
303 YLYLSRTNTPSGTTTQSRLLQFSQAGASDIRDQSRNWLPGPCYRQQRVSKTSADNNNSEYSWTGATKYHLNGRDSLVPNGPAMASHKDEEKFFPQSGVLIFGK 406
407 QKSEKTNVDIEKVMITDEEEIRTTNPVATEQYGSVSTNLQQRNRQAATADVNTQGVLPGMVWQDRDVLVYQGPWAKIPHTDGHFHPSPLMGGFGLKHPPPQILI 510
511 KNTVPANPSTTFSAAKFASFITQYSTGQVSVEIEWELQKENSKRWNPEIQYTSNYNKSVMVDFTVDTNGVYSEPRPIGTRYLTRNL C-term 597
  
```

C:VP3 Monoisotopic mass: 59936.8685 Average mass: 59974.6971 Molecular formula: C2661H3984N740O824S14

```

1 N-term ATGSGAPMADNNEGADGVGNSSGNWHCDSTWMDRVIITSTRTWALPTYNNHLYKQISSQSGASNDNHYFGYSTPWGYDFNRFHCHFSPRDWQ 94
95 RLINNNWGFRPKRLNFKLFNIQVKEVTQNDGTTIANNLTSTVQVFTDSEYQLPYVLGSAHQGCLPPFPADVFMVPOYGYLTLNNGSQAVGRSSFYCLEYFPSQ 198
199 MLRTGNNTFTFSYTFEDVPPHSSYAHSQSLDRLMNPLIDQYLYLSRTNTPSGTTTQSRLLQFSQAGASDIRDQSRNWLPGPCYRQQRVSKTSADNNNSEYSWTGA 302
303 TKYHLNGRDSLVPNGPAMASHKDDEEKFFPQSGVLIFGKQSEKTNVDIEKVMITDEEEIRTTNPVATEQYGSVSTNLQQRNRQAATADVNTQGVLPGMVWQDR 406
407 DVYLQGPWAKIPHTDGHFHPSPLMGGFGLKHPPPQILIKNTVPANPSTTFSAAKFASFITQYSTGQVSVEIEWELQKENSKRWNPEIQYTSNYNKSVMVDFT 510
511 VDTNGVYSEPRPIGTRYLTRNL C-term 532
  
```

Figure 2. Primary amino acid sequence of AAV-2 capsid proteins. Shown in Agilent MassHunter Sequence Manager software, VP1–3 differ only in their N-terminal sequences: each contains the VP3 sequence, with an additional N-terminal sequence underlined in red (VP2) or red and green (VP1). The monoisotopic mass, average mass, and molecular formula are shown above for each protein.

As published elsewhere,⁵ these post-translational modifications were anticipated: (i) removal of the initiator methionine on VP1 and VP3, and (ii) acetylation of the amino acid immediately following the removed methionine. Acetylated amino acids were indicated in Agilent MassHunter Sequence Manager software as red, italicized letters, and the theoretical average masses of VP1–3 were 81,856.13, 66,488.91, and 59,974.70 Da respectively (Figure 2).

Denatured AAV-2 samples were separated on ZORBAX RRHD 300Å SB-C3, SB-Diphenyl and SB-C18 columns (Figures 3A to 3C) using the Testing gradients shown in Table 1. VP1–3 separated as two peaks on SB-C3 and SB-Diphenyl columns, with VP1 and VP3 coeluting as a single peak. Only the SB-C18 column possessed the selectivity necessary to separate each capsid protein.

Deconvoluted mass spectra of the VP1 + VP3 peak (Figures 3D to 3E) showed a far more intense VP3 signal at 59,975.52 Da compared to VP1, reflecting its order of magnitude greater abundance. The coelution of VP3 may constitute a matrix effect, potentially interfering with detection and mass accuracy of VP1 through ion suppression.⁸ In contrast, the superior separation of VP1 on the SB-C18 column (Figure 3F) greatly reduced interference by VP3, permitting reliable and accurate mass spectrometry analysis of VP1.

As shown in Figure 4, AAV-2 samples were then separated on a SB-C18 column using the optimized gradient shown in Table 1, improving peak resolution and shape and shortening analysis time. Note that the slight background undulation in the total ion current was likely caused by residual Pluronic F-68, which did not interfere significantly with the analysis.

Importantly, the observed deconvoluted mass of VP1 was 81,885.72 Da (Figure 4E), which was +29.6 Da greater than the theoretical value of 81,856.13 Da. In contrast, the observed masses of VP2 and VP3 were in good agreement with their theoretical values. Therefore it was hypothesized that a single amino acid substitution had occurred in the N-terminal region of VP1 (sequence underlined in green, Figure 2).

Confirmation of single amino acid substitution in AAV-2

A tryptic digestion and peptide mapping of AAV-2 was performed to test this hypothesis. Identification was made of a triply charged 1,102.1864 *m/z* peptide whose MS/MS spectrum confirmed an alanine → threonine substitution at amino acid 77 of the VP1 sequence, which was indeed located in the N-terminal region (Figure 5).

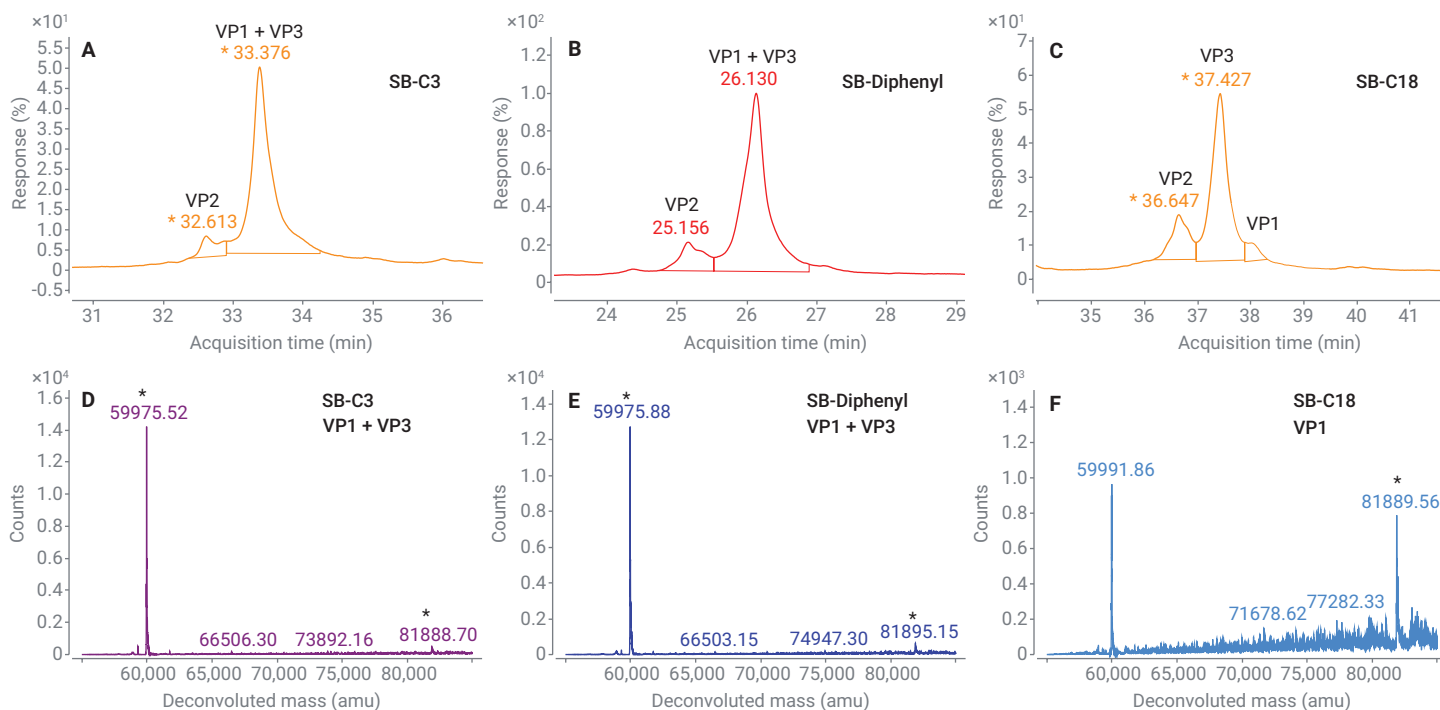


Figure 3. Method development with AAV-2. Fluorescence chromatograms depicting separation using (A) Agilent ZORBAX RRHD 300Å SB-C3, (B) SB-Diphenyl, and (C) SB-C18 columns. Note the superior chromatographic resolution of SB-C18. (D to F) Deconvoluted mass spectra of chromatographic peaks showing the coelution of VP1 and VP3.

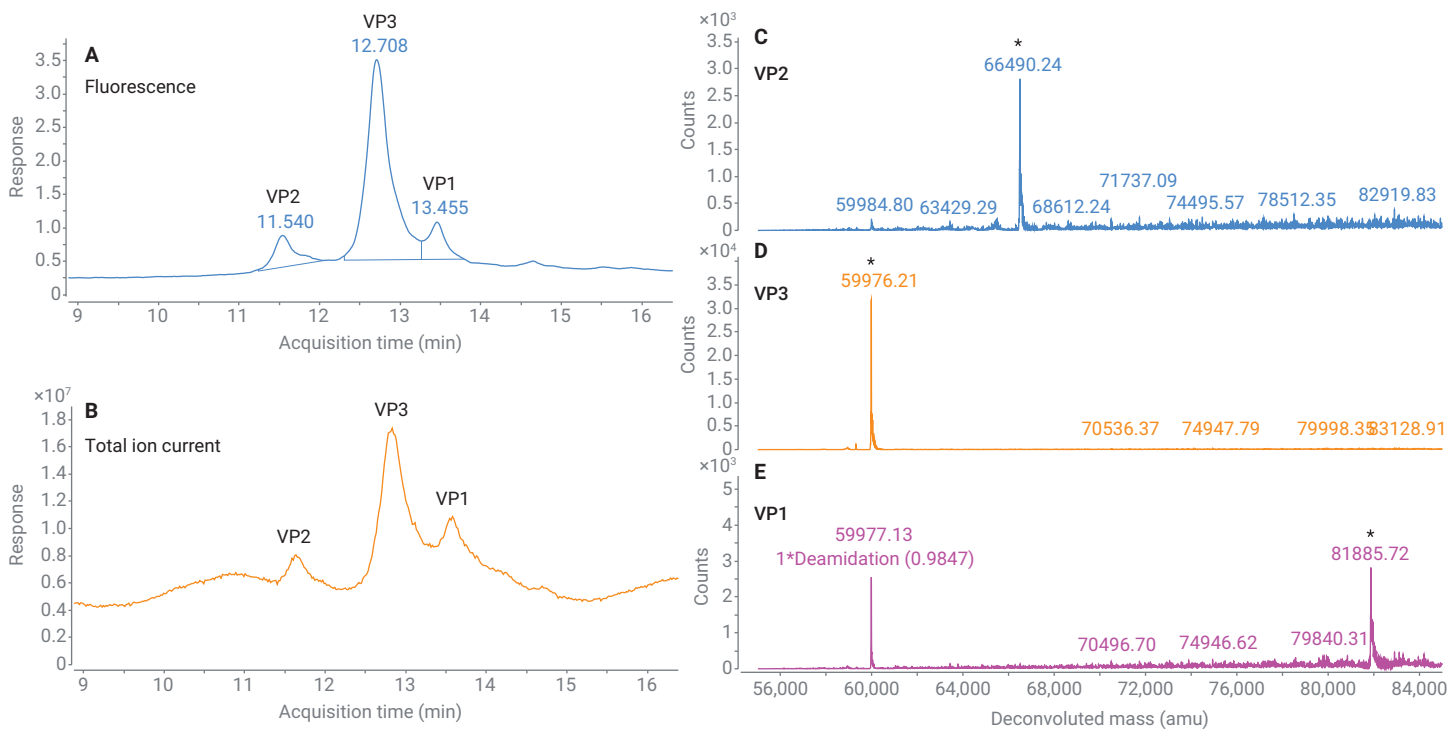


Figure 4. LC/MS of denatured AAV-2 capsid proteins using the optimized method on an Agilent ZORBAX RRHD 300Å SB-C18 column. (A) Fluorescence chromatogram depicting the three capsid proteins. (B) Total ion current. (C to E) Deconvoluted mass spectra of the three capsid proteins, with the relevant mass peaks marked by asterisks.

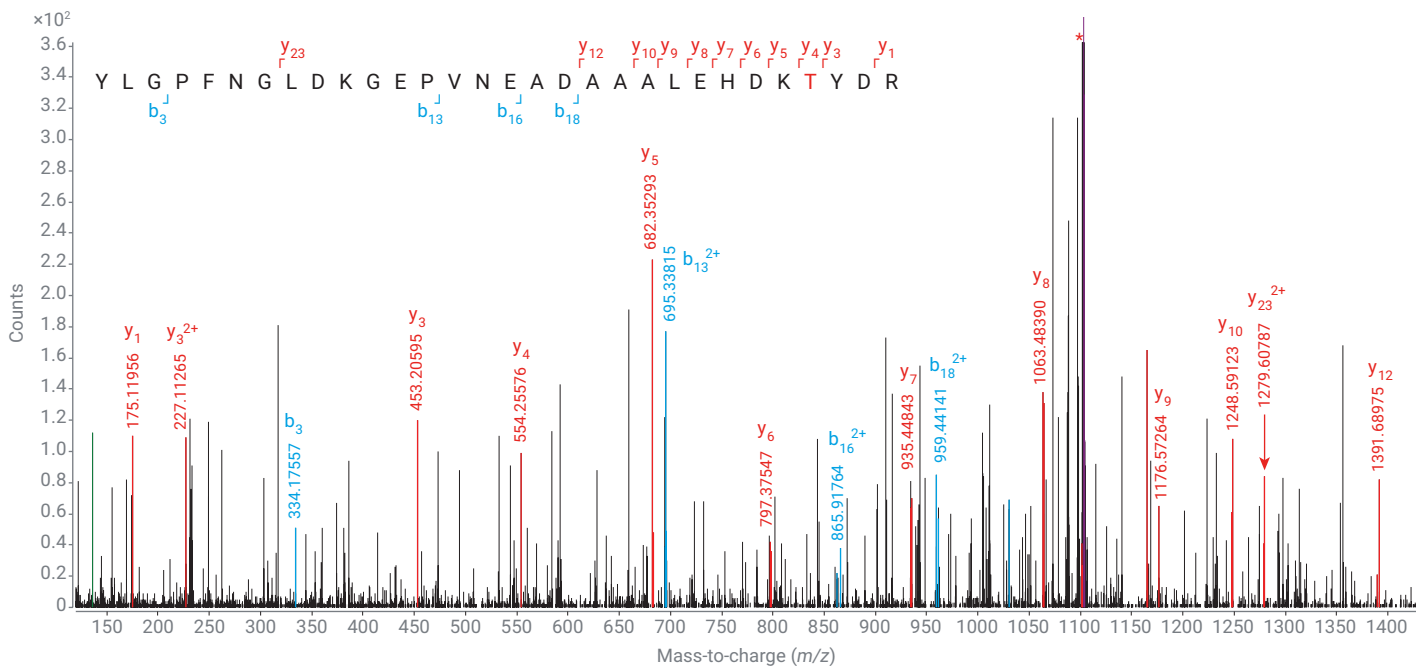


Figure 5. Confirmation of alanine \rightarrow threonine substitution in VP1 by MS/MS. The substituted amino acid is shown in red font, and the precursor ion is marked by a red asterisk.

Orthogonal confirmation of this mutation was obtained by Sanger sequencing of the plasmid used for AAV-2 expression, which showed that a G → A substitution had altered a GCC codon to ACC (data not shown).

Analysis of six additional AAV serotypes

To assess the generalizability of this LC/MS method to the analysis of other AAV serotypes, AAV-7, 7m8, DJ, 9, rh10, and Anc80 were analyzed using the

optimized SB-C18 method described above. AAV-7, 7m8 and DJ separated well using this method (Figures 6A to 6C), but AAV-9, rh10, and Anc80 separated as only two peaks, with VP1 and VP3 coeluting as single peaks.

Agilent diphenyl stationary phases have altered selectivity compared to alkyl chain stationary phases such as C3, C8, and C18. The phenyl groups permit separation based on π - π interactions with additional affinity for aromatic

amino acids and double bonds.⁹ An optimized SB-Diphenyl method (Table 1) was developed to achieve successful separation of AAV-9, rh10, and Anc80 (Figures 6D to 6F). The identity of each capsid protein was automatically matched by BioConfirm software using the deconvoluted mass spectrum from each peak, which showed minimal interference from neighboring peaks (Figures 7 and 8).

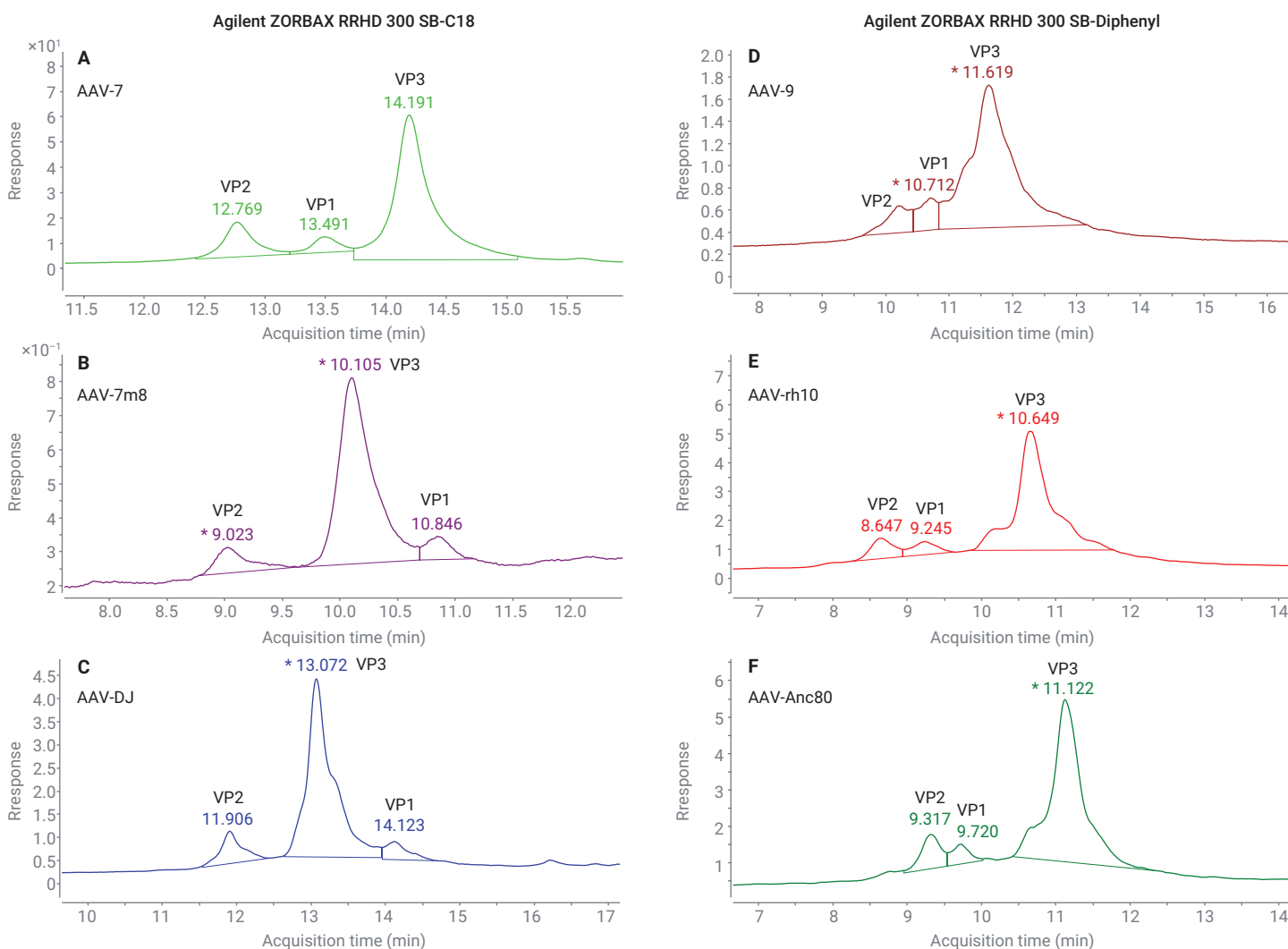


Figure 6. LC/MS of denatured AAV capsid proteins of six different serotypes on (A to C) Agilent ZORBAX RRHD 300 SB-C18, and (D to F) Agilent SB-Diphenyl columns.

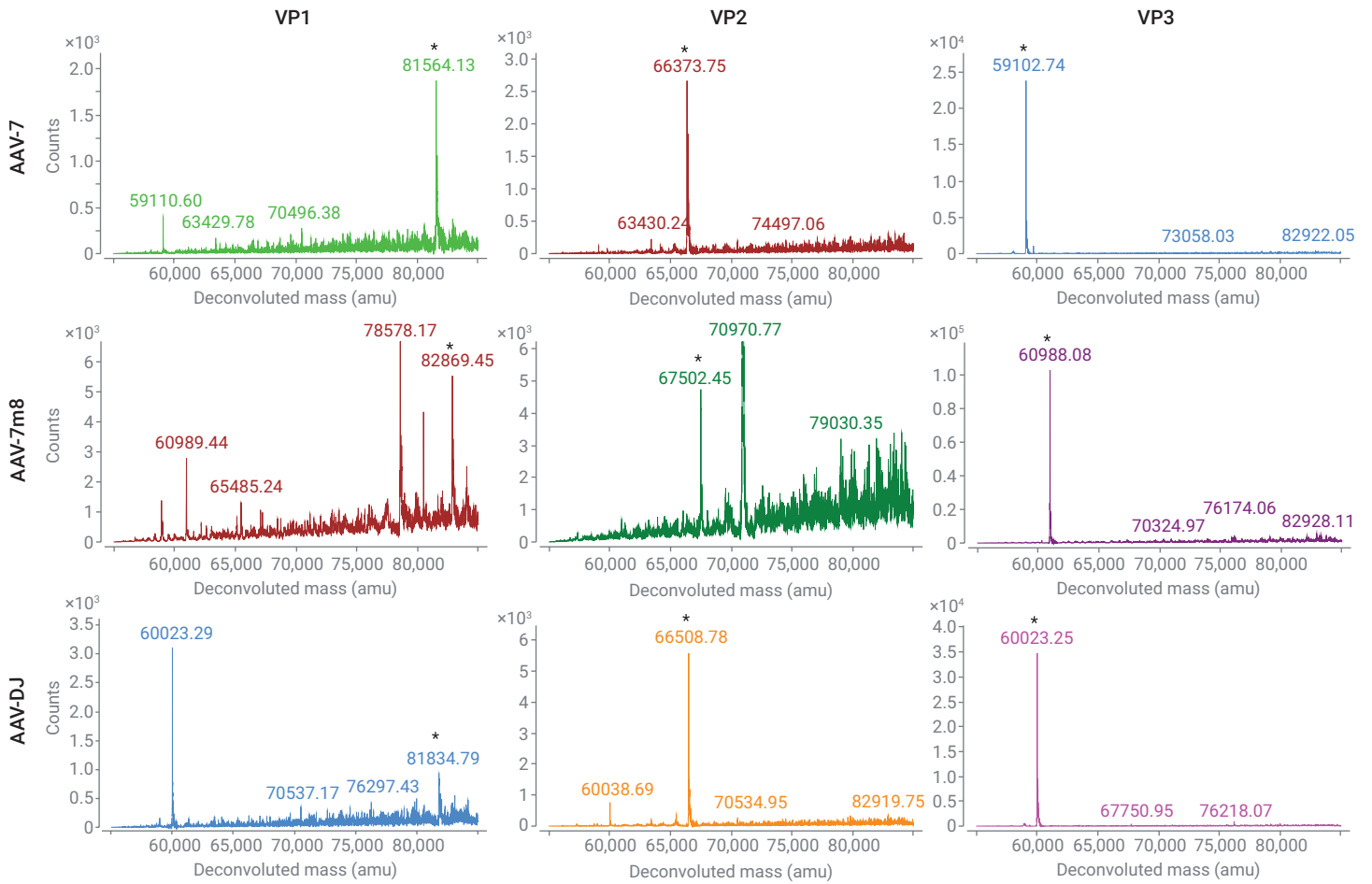


Figure 7. Deconvoluted mass spectra of AAV capsid proteins separated on an Agilent ZORBAX RRHD 300 SB-C18 column. Some interference from coeluting host cell proteins was seen in AAV-7m8 (70971.71, 78578.01, and 80495.10 Da).

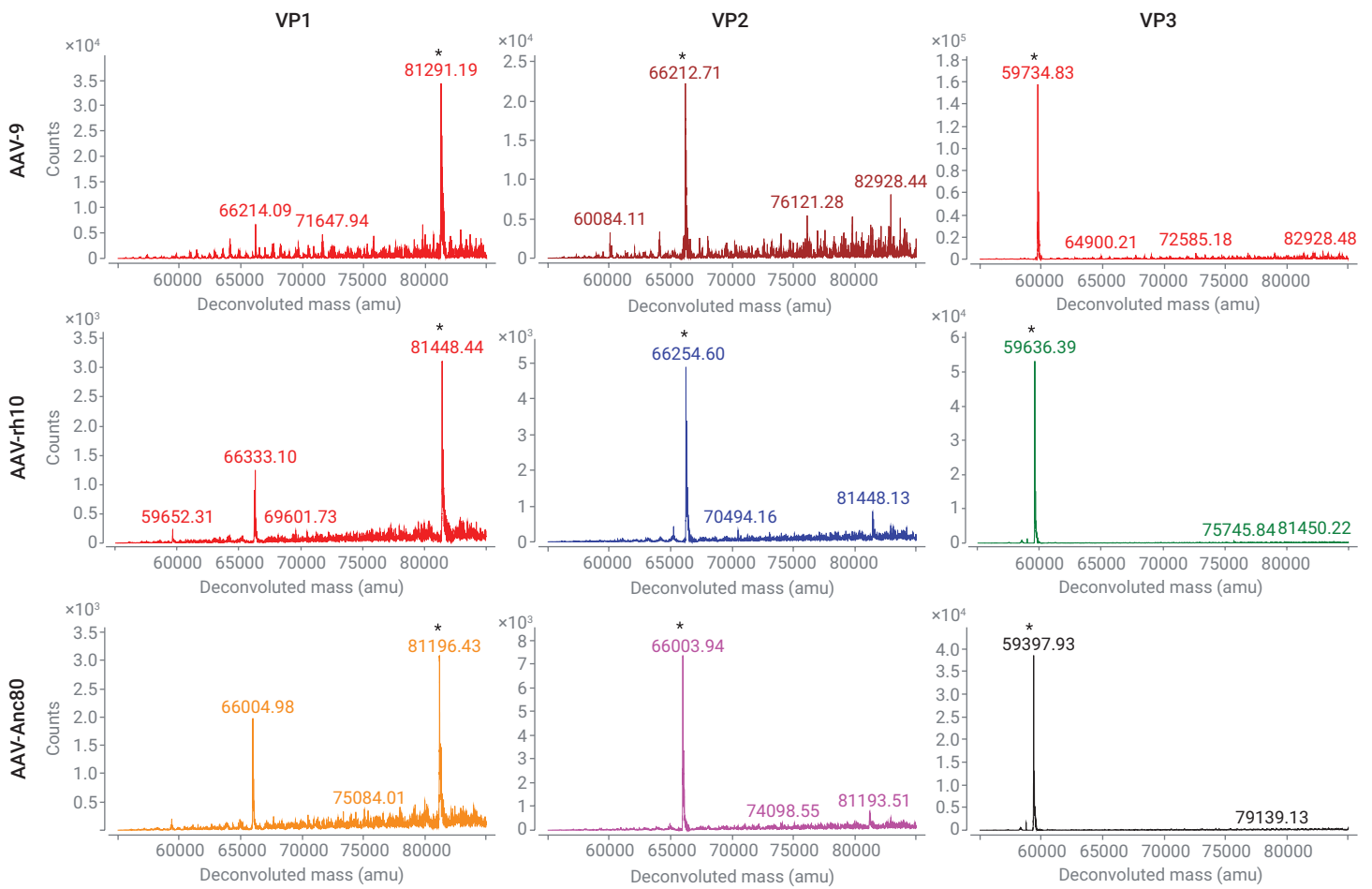


Figure 8. Deconvoluted mass spectra of AAV capsid proteins separated on an Agilent ZORBAX RRHD 300 SB-Diphenyl column.

Deamidations were putatively assigned to VP1 proteins of AAV-DJ and rh10, which could be due to cell culture conditions or generated during sample preparation as artifacts of heating. Except for AAV-2, the theoretical and observed masses for each capsid protein (Table 6) differed by ≤ 3 Da, corresponding to ≤ 32 ppm.

The relative quantities of VP1–3 in Table 7 were measured by integrating the fluorescence chromatogram peaks (Figure 6) corresponding to each capsid protein. While these results generally conformed to the expected VP1:2:3 stoichiometry of 1:1:10, the abundance of VP1 appeared to be more variable than VP2 across the different samples

tested. As VP1 is known to be a critical nuclear localization factor,¹⁰ the lower abundance of VP1 in some samples may partially account for differences in infectivity.

Table 6. Deconvoluted masses of capsid proteins.

AAV Capsid Protein Masses									
Serotype	VP1			VP2			VP3		
	Theoretical	Observed	Mass Accuracy (ppm)	Theoretical	Observed	Mass Accuracy (ppm)	Theoretical	Observed	Mass Accuracy (ppm)
2	81886.16	81885.72	5.37	66488.91	66490.24	20.00	59974.70	59976.21	25.18
7	81564.08	81564.13	0.61	66372.17	66373.75	23.81	59101.05	59102.74	28.60
9	81291.57	81291.19	4.67	66210.77	66212.71	29.30	59733.54	59734.83	21.60
7m8	82868.27	82869.45	14.24	67501.05	67502.45	20.74	60986.83	60988.08	20.50
DJ	81835.21	81834.79	5.13	66508.06	66508.78	10.83	60021.86	60023.25	23.16
rh10	81445.85	81448.44	31.80	66252.96	66254.60	24.75	59634.58	59636.39	30.35
Anc80	81195.42	81196.68	15.52	66002.53	66003.80	19.24	59396.22	59397.97	29.46

Table 7. Relative quantities of capsid proteins.

Capsid Protein Quantification (FLD %)			
Serotype	VP1	VP2	VP3
2	10.67	10.61	78.72
7	7.16	9.81	83.03
9	8.75	8.04	83.21
7m8	7.62	9.70	82.68
DJ	8.62	11.72	79.66
rh10	6.58	9.18	84.24
Anc80	5.64	10.62	83.74

Conclusion

This application note shows the development of the method for the efficient separation of intact AAV capsid proteins using the 1290 Infinity II LC in conjunction with ZORBAX RRHD 300Å SB-C18 or SB-Diphenyl columns, followed by subsequent detection and analysis using a 1260 Infinity II fluorescence detector in tandem with a 6545XT AdvanceBio LC/Q-TOF. This application note demonstrates the capabilities of this method with seven different AAV serotypes. Only a relatively short denaturation step was required for sample preparation, and no buffer exchange was required because the method was robust to high salt conditions as well as the common detergent additive Pluronic F-68.

This method significantly outperformed recent published efforts⁵ in terms of chromatographic separation, and represents a more general approach to the efficient separation of AAV capsid proteins, which may coelute with one column chemistry, but resolve well on another. In comparison to another recent effort using a ZipChip CE/MS system for a similar analysis,¹¹ this approach achieves mass accuracy of ≤ 32 ppm compared to ≤ 60 ppm for the ZipChip. In addition, the relatively long retention time differences achieved by liquid chromatography facilitated accurate and reproducible mass spectral deconvolution, and the inclusion of a fluorescence detector permitted sensitive and accurate relative quantitation of capsid protein abundance. In contrast, capsid proteins were shown to elute within a narrow 0.1-minute time window on the ZipChip, with the relatively slow scan rate of the mass spectrometer used in the experiment precluding accurate quantitation.

It is anticipated that this method will be useful for rapid confirmation of AAV product identity before release, as well as in screening AAV mutant libraries in discovery/development laboratories.

References

1. Keeler, A. M.; Flotte, T. R. Recombinant Adeno-Associated Virus Gene Therapy in Light of Luxturna (and Zolgensma and Glybera): Where Are We, and How Did We Get Here? *Annu. Rev. Virol.* **2019**, *6*, 601–621.
2. Backovic, A. *et al.* Capsid Protein Expression and Adeno-Associated Virus like Particles Assembly in *Saccharomyces Cerevisiae*. *Microb. Cell Fact* **2012**, *11*, 124.
3. Chemistry, Manufacturing, and Control (CMC) Information for Human Gene Therapy Investigational New Drug Applications (INDs) - Guidance for Industry. *US Food and Drug Administration* **2020**.
4. Kuck, D.; Kern, A.; Kleinschmidt, J. A. Development of AAV Serotype-Specific ELISAs Using Novel Monoclonal Antibodies. *Journal of Virological Methods* **2007**, *140*, 17–24.
5. Jin, X. *et al.* Direct Liquid Chromatography/Mass Spectrometry Analysis for Complete Characterization of Recombinant Adeno-Associated Virus Capsid Proteins. *Human Gene Therapy Methods* **2017**, *28*, 255–267.
6. Bosma, B. *et al.* Optimization of Viral Protein Ratios for Production of RAAV Serotype 5 in the Baculovirus System. *Gene Therapy* **2018**, *25(6)*, 415–424.
7. Rehder, D. S. *et al.* Reversed-Phase Liquid Chromatography/Mass Spectrometry Analysis of Reduced Monoclonal Antibodies in Pharmaceuticals. *J. Chromatog. A* **2006**, *1102(1–2)*, 164–175.
8. Matuszewski, B. K.; Constanzer, M. L.; Chavez-Eng, C. M. Strategies for the Assessment of Matrix Effect in Quantitative Bioanalytical Methods Based on HPLC-MS/MS. *Analytical Chemistry* **2003**, *75(13)*, 3019–3030.
9. Long, W. J.; Mack, A. E. Comparison of Selectivity Differences Among Different Agilent ZORBAX Phenyl Columns Using Acetonitrile or Methanol. *Agilent Technologies application note*, publication number 5990-4711EN, **2009**.
10. Popa-Wagner, R. *et al.* Impact of VP1-Specific Protein Sequence Motifs on Adeno-Associated Virus Type 2 Intracellular Trafficking and Nuclear Entry. *Journal of Virology* **2012**, *86*, 9163–9174.
11. Zhang, Y. *et al.* Identification of Adeno-Associated Virus Capsid Proteins Using ZipChip CE/MS. *Analytical Biochemistry* **2018**, *555*, 22–25.

www.agilent.com/chem

RA.5878472222

This information is subject to change without notice.

© Agilent Technologies, Inc. 2020, 2021
Printed in the USA, January 27, 2021
5994-2434EN

